Supplementary Information for

A Simple and Efficient Hydrogen Production-Storage Hybrid Material System (Co/TiO$_2$) for Synchronizing Hydrogen Photogeneration with Uptake

Yurong Yang,[b,c] Peng Gao,*[a,b] Ying Wang,[b] Linna Sha,[b] Xiaochen Ren,[b] Jianjiao Zhang,[b] Piaoping Yang,*[b] Tingting Wu,[b] Yujin Chen*[d] and Xiaobo Li[b]

Characterization

X-ray diffraction (XRD) patterns of the samples were recorded by a D/MAX2500 diffractometer equipped with Cu K*α* radiation (λ=0.15406 nm). Diffraction patterns were collected from 10° to 70° at a scan rate of 10 ^oC min^{-1}. The field emission scanning electron microscopy (FE-SEM) images were taken on a SU8000 cold emission field scanning electron microanalyser (Hitachi, Japan). Transmission electron microscopy (TEM), high-resolution transmission electron microscopy (HRTEM) and scanning transmission electron microscopy with an energy dispersive X-ray spectroscopy (STEM-EDS) experiments were performed on a JEOL 2010 transmission electron microscope with a field emission gun operated at 200 kV. X-ray photoelectron spectroscopy (XPS) examination was performed by using a PHI 5700 ESCA System with a monochromatic Al Kα (1486.6 eV) radiation source and a hemisphere detector. Raman spectroscopic analysis was performed by using a micro-Raman system with an Ar ion laser 488 nm, and a probing laser 50 W cm^{-2} was guided during the illumination. The ultraviolet–visible diffuse reflectance spectrum (UV-vis DRS) measurements were conducted using a UV-vis spectrophotometer (Shimadazu, UV-2550) with $BaSO_4$ as the reference sample. Fourier transform infrared (FTIR) spectra of the products were recorded on a Perkin-Elmer 580B IR spectrophotometer using the KBr pellet technique. Brunauer-Emmett-Teller (BET) nitrogen adsorption-desorption measurements (Micromeritics TriStar 3020) were carried out to determine the as-prepared samples' specific surface area at 77 K. The room-temperature photoluminescence (PL) spectrum was measured using a spectrophotometer (Jobin Yvon Fluorolog 3-221) with a Xe lamp (450 W) as excitation source at the excitation wavelength of 320 nm. Zeta potential distribution was performed on a ZEN3690 Zetasizer Nano detector (Malven, UK). Thermogravimetric experiments were conducted by using thermo-gravimetric (TG, Diamond–Pyris) analysis from room temperature to 800 ^{o}C at a rate of 10 ^{o}C min^{-1}. Hydrogen release from sample was confirmed by a temperature programmed desorption (TPD, TP-5080) analysis from room temperature to 800 ^{o}C at a rate of 10 ^{o}C min^{-1} under argon gas. The desorbed hydrogen from sample was analyzed by the mass spectrometer (MS, HIDEN-QIC-20). TPD and MS signals were recorded simultaneously.

Photo-electrochemical measurements

1.0 mg as-prepared sample was dispersed in 1 mL ethanol, and then it was uniformly spin-dropped onto a 1 cm×1 cm FTO glass substrate by a spin coater (VTC-50A, China). Subsequently, the glass was heated at 60 ^{o}C in a vacuum oven for 10 hours.

The photocurrent measurements were recorded on a semiconductor characterization system (Keithley 4200 SCS) with a Lakeshore probe station and a xenon lamp (300 W, λ>400 nm) was used as the visible-light source.

Electrochemical impedance spectroscopy (EIS) measurements were performed on a CHI 660D electrochemical station (Shanghai Chenhua) with a three-electrode system, in which Pt foil and saturated Ag/AgCl were used as the counter electrode and reference electrode, respectively. And the electrolyte was 1 M Na_2SO_4 solution bubbled with N_2 for 30 min before the measurements.

Measurement of photocatalytic hydrogen evolution

The photocatalytic hydrogen production experiments were performed in a 500 mL closed quartz flat-bottom container. Firstly 100 mg catalyst powder was dispersed in a 100 mL aqueous solution, which contained 80 mL distilled water and 20 mL methanol. A 300 W xenon arc lamp was used as a visible light source to trigger the photocatalytic reaction. The power density of the incident light was 180 mW cm^{-2}, which was measured by a CEL-HFX300 Visible spectrophotometer. The amount of H_2 evolution was measured using an on-line gas chromatograph (SP7800, TCD, molecular sieve 0.5 nm, N_2 carrier, Beijing Keruida Limited).

Calculation of hydrogen storage capacity of metal Co

The hydrogen storage capacity of metal Co is calculated using the Equation:

$$\eta = \frac{M_{H_2}.(v_H.t_H)}{C_{Co}} \times 100\% \qquad (1)$$

where η is the ratio of stored hydrogen to metal Co in the sample, M_{H_2} is the molar mass of hydrogen, υ_H the H_2 evolution rate of 1g sample, t_H is the H_2 evolution time(from the begin time of photocatalytic reaction to the time of detecting hydrogen), and C_{Co} is the mass percentage of cobalt in the sample. Moreover, based on the TG measurement, the weight losses (~0.4%) of Co/TiO_2 NTs under a higher temperature (>440 ^{o}C) after photocatalytic reaction is due to a release of hydrogen. The hydrogen storage capacity of metal Co is also calculated using the Equation:

$$\eta = \frac{m.\eta_L}{mC_{Co}} \times 100\% = \frac{\eta_L}{C_{Co}} \times 100\% \qquad (2)$$

Where η is the ratio of stored hydrogen to metal Co in the sample, *m* is the weight of the sample, η_L is the weight loss of the sample, and C_{Co} is the mass percentage of cobalt in the sample.

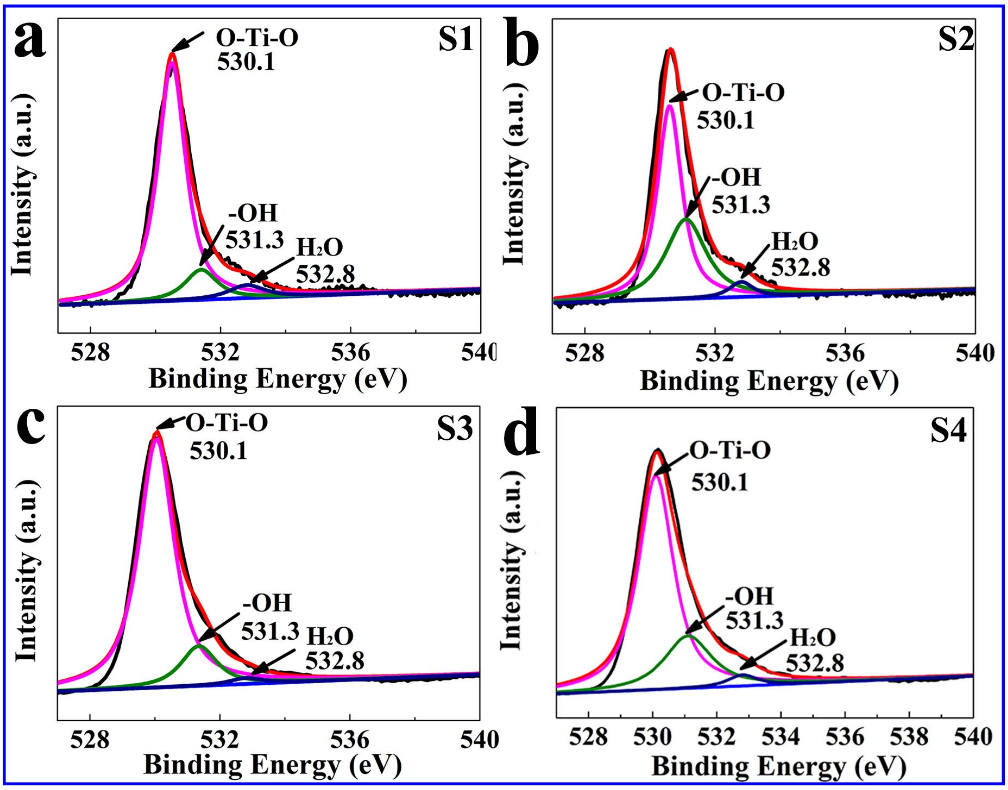

Figure S1. XPS O 1s spectra of Co/TiO_2 samples.

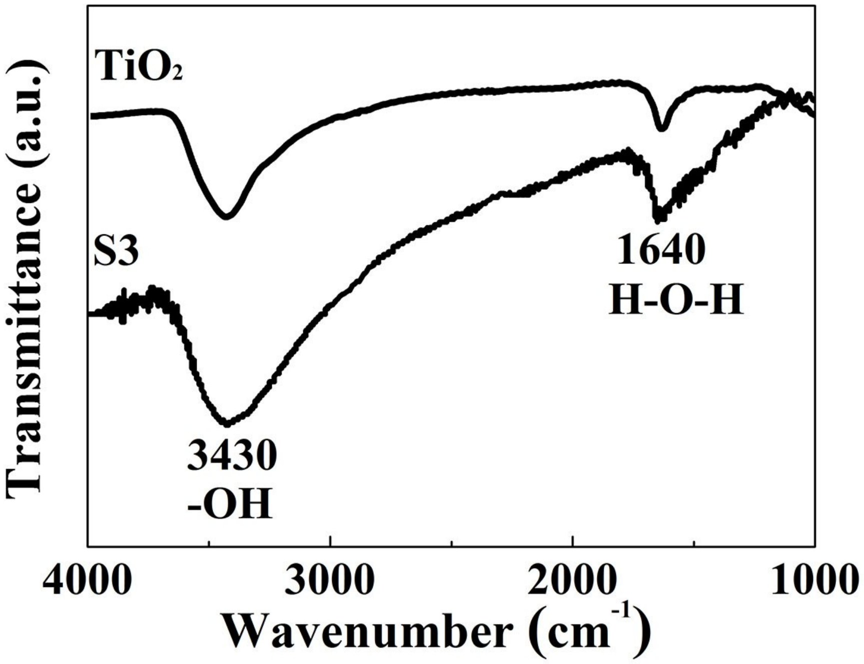

Figure S2. FTIR spectra of TiO_2 NTs and sample S3.

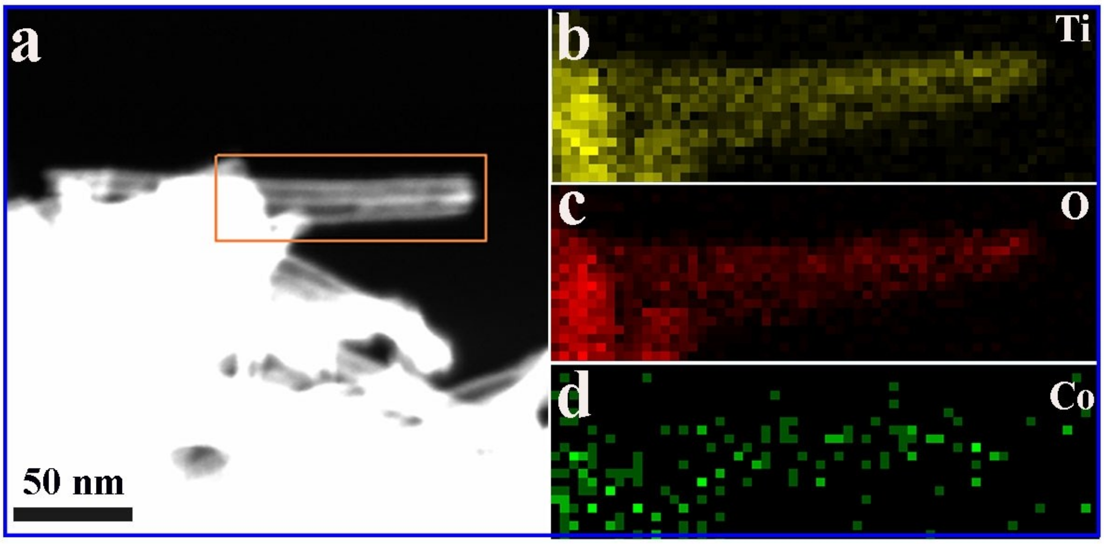

Figure S3. TEM image of sample S1 and its corresponding EDS element mappings of Ti, O and Co elements.

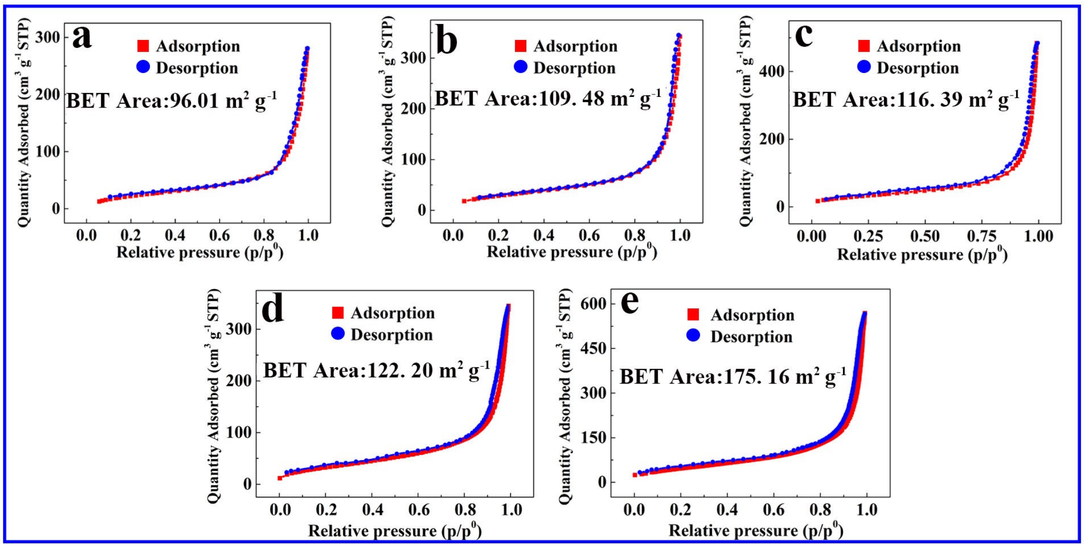

Figure S4. Nitrogen adsorption-desorption isotherms of TiO_2 precursor (a), sample S1 (b), sample S2 (c), sample S3 (d) and sample S4 (e).

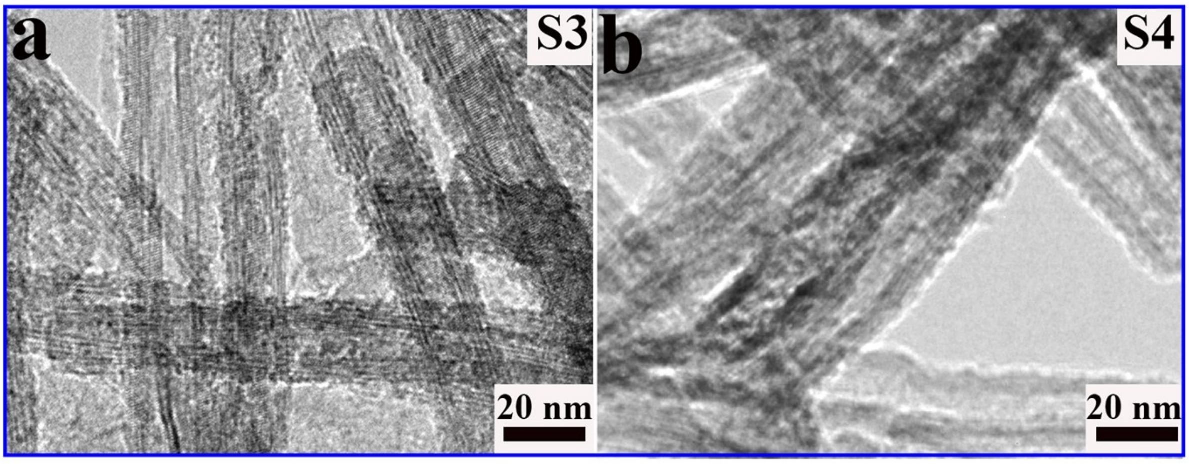

Figure S5. TEM images of sample S3 (a) and sample S4 (b).

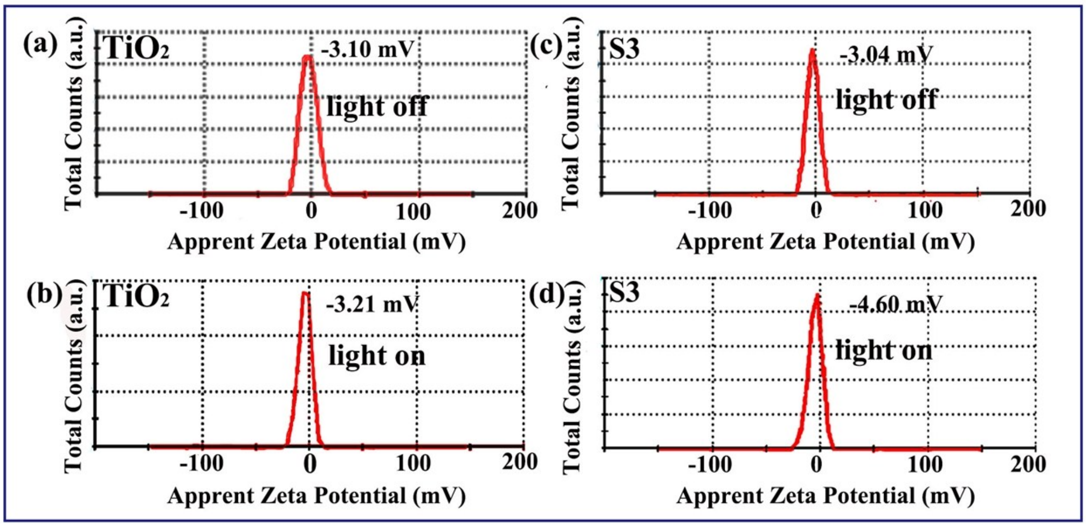

Figure S6. The zeta potentials of TiO_2 precursor (a, b) and sample S3 NTs (c, d) under on/off light.

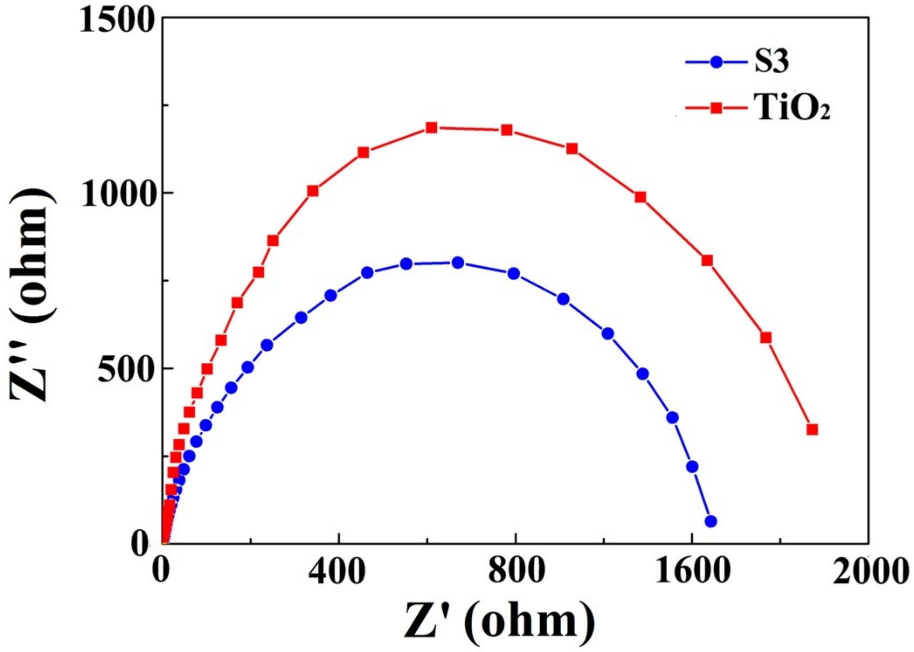

Figure S7. EIS Nyquist plots of TiO_2 precursor and sample S3.

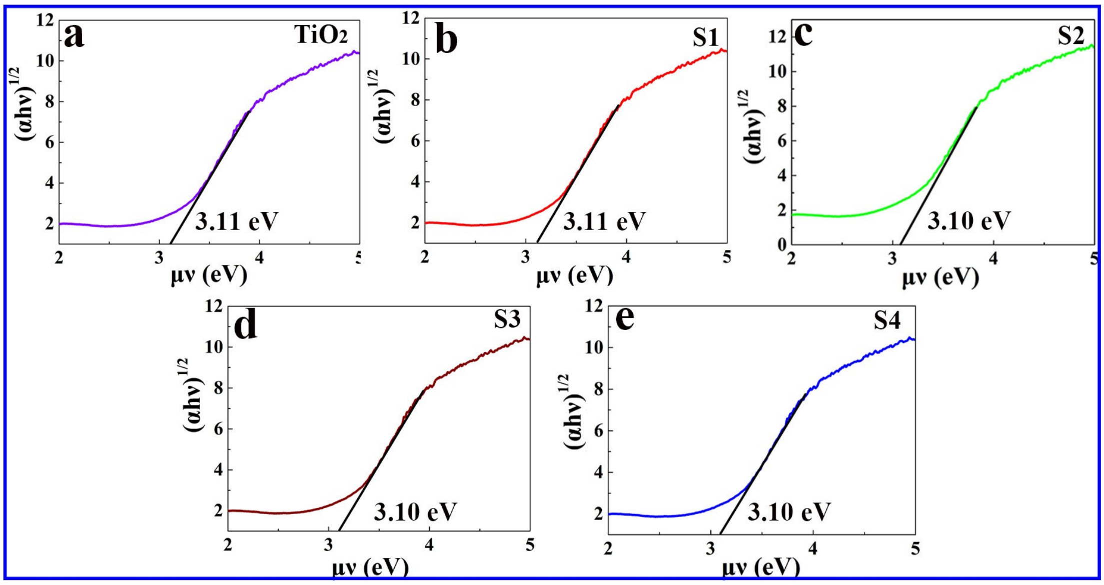

Figure S8. Optical band gaps determined by the UV-vis DRS of TiO_2 NT precursor (a), sample S1 (b), sample S2 (c), sample S3 (d) and sample S4 (e).

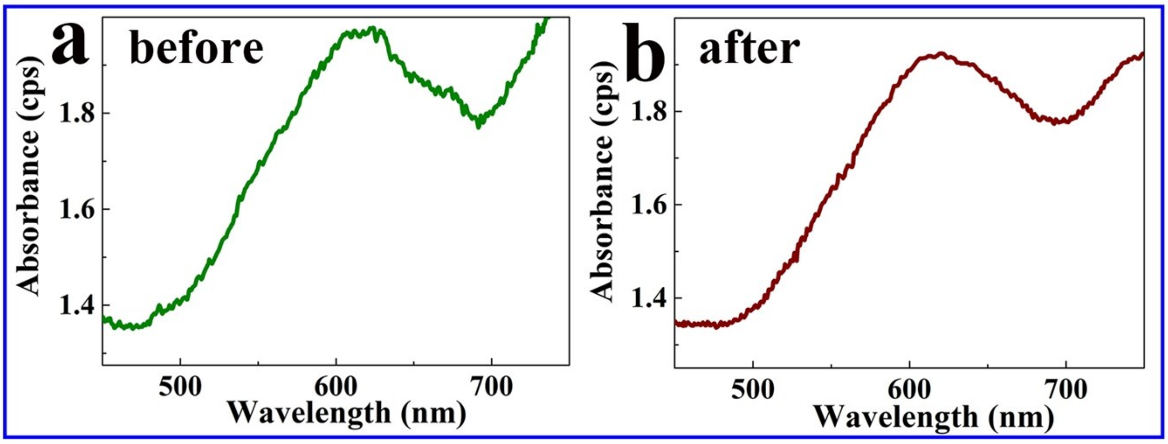

Figure S9. UV-vis DRS spectra of sample S3 before (a) and after (24 hours) the photocatalytic water splitting (b).

UV-vis DRS spectra of S3 NTs before and after the photocatalytic water splitting are shown in Figure S9. After the photocatalytic water splitting for H_2 production, the absorption in the visible light region of sample S3 is almost unchanged.

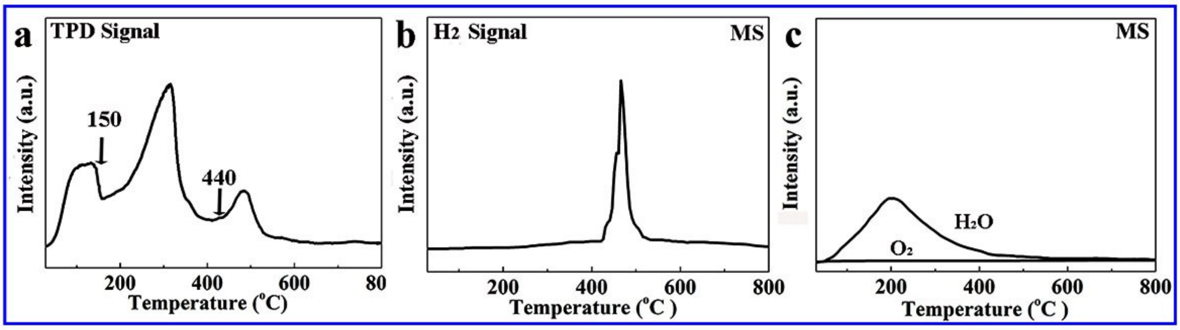

Figure S10. TPD (a) and H_2 (b), H_2O and O_2 (c) signals of the sample S3 after the photocatalytic water splitting.

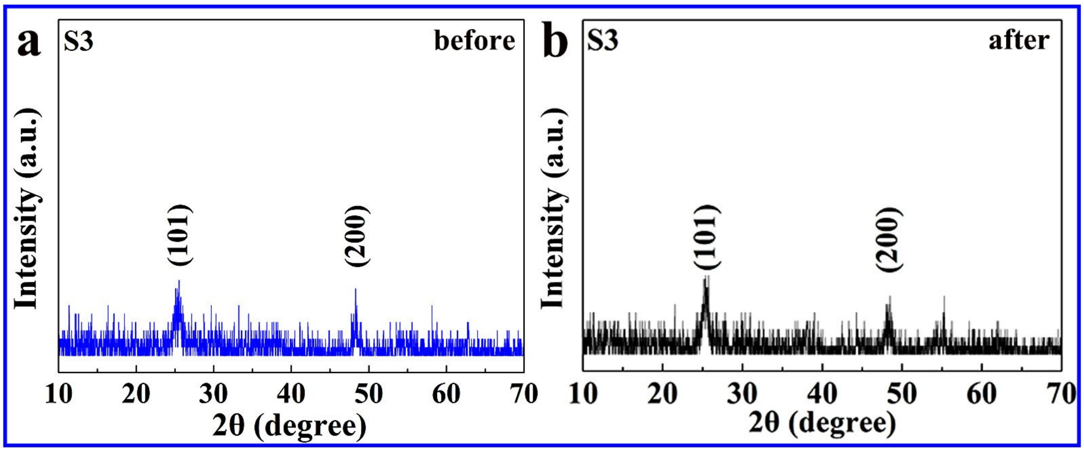

Figure S11. XRD patterns of sample S3 before (a) and after (24 hours) the photocatalytic water splitting (b).

XRD patterns of sample S3 NTs before and after the photocatalytic water splitting are shown in Figure S11. After the photocatalytic water splitting for H_2 production, the amorphous state of Co is unchanged.

Table S1. The element mass percentage of sample S3

Element	Ti	O	Co
Atomic percentage (%)	31.24	62.49	6.27
Mass percentage (%)	52.22	34.89	12.89